

PSInSAR Processing for Volcanic Ground Deformation Monitoring Over Fogo Island [†]

Arun Babu * and Shashi Kumar

Photogrammetry and Remote Sensing Department, Indian Institute of Remote Sensing, ISRO, Dehradun 248001, India; shashi@iirs.gov.in

* Correspondence: arunlekshmi1994@gmail.com; Tel.: +91-807-546-6497

[†] Presented at the 2nd International Electronic Conference on Geosciences, 8–15 June 2019; Available online: <https://iecg2019.sciforum.net/>.

Published: 5 June 2019

Abstract: Persistent Scatterer Interferometry Synthetic Aperture Radar (PSInSAR) has been widely used in the precise measurement of ground deformation due to anthropogenic and natural disturbance of the earth's surface. The present study has utilized the spaceborne C-band Sentinel-1 data for PSInSAR processing to generate a displacement map due to the volcanic eruption of Pico do Fogo volcano of the Fogo Island. An eruption was recorded in the year 2014–2015 and the Fogo volcano became active on 23 November 2014. It was observed that the intensity of the volcanic eruption during 2014–2015 had approached the intensity of the volcanic eruption of 1951, which was recorded as one of the strongest eruptions on the island. The volcanic eruption continued for 77 days and it stopped on 8 February 2015. To find the mean line-of-sight displacement from PSInSAR processing, a total of seven Single Look Complex (SLC) products of Sentinel-1 data in the interferometric mode were used. The SLC product of the SAR data that was acquired before the start of the volcanic eruption was chosen as the master image and all the remaining six slave images were precisely coregistered. The selection of Persistent Scatterers (PSs) is the most important step in PSInSAR processing. The initial set of PSs was identified by amplitude stability index and phase analysis was performed to estimate the phase stability of each resolution cell. After PS identification, 3D phase unwrapping was performed. The unwrapping step involved the low-pass filtering of the complex phase difference and time series in the frequency domain using a Gaussian window. The phase difference between each filtered data point was then calculated. The unwrapped phase of the interferogram was used to generate a displacement map for the volcanic field. The PSInSAR-based line-of-sight displacement was measured in the range of -34 mm to $+35$ mm and the standard deviation of the displacement ranged from $+2$ mm to $+30$ mm.

Keywords: PSInSAR; Interferometric Wide; amplitude dispersion index; deformation

1. Introduction

Persistent Scatterer Interferometry is an advanced Synthetic Aperture Radar (SAR) interferometric technique capable of estimating surface deformations with millimetre-level accuracy [1]. Conventional Interferometric SAR (InSAR) has the potential to estimate surface deformations. However, the high temporal decorrelation in the interferograms caused by vegetation limits the capability of InSAR to estimate the deformation of natural terrains. The accuracy of the InSAR is also affected by the phase delay introduced by the atmospheric constituents, which are difficult to remove from the interferograms [2]. The PSInSAR technique utilizes a large number of interferometric pairs, compared to InSAR, to overcome these limitations. Persistent Scatterers are the ground targets, which exhibit amplitude and phase stability in all the datasets. PSInSAR uses these

stable scatterers to effectively estimate and remove the atmospheric and topographic artifacts from the interferograms. The resulting differential interferograms contain only the residual phase due to surface deformations [3]. The PSInSAR technique has proven potential for volcanic deformation estimation [4,5].

Pico do Fogo, on Fogo Island (Figure 1 published by [6]), is the most active volcano and the highest peak in the Cape Verde archipelago and in the Central Atlantic oceanic region. It was formed as the African Plate moved towards the east over the hotspot and is the youngest volcano in the Cape Verde Islands. There have been roughly 26 eruptions in the past 500 years [7]. Fogo erupted on 23 November 2014, breaking its 20 years of quiescence since 1995. The eruption lasted for 77 days until February 2015, causing massive destruction to the nearby areas. On 28 November 2014, the lava flow through a linear fissure completely destroyed the Portela and Bangaeria villages near the volcano [6].

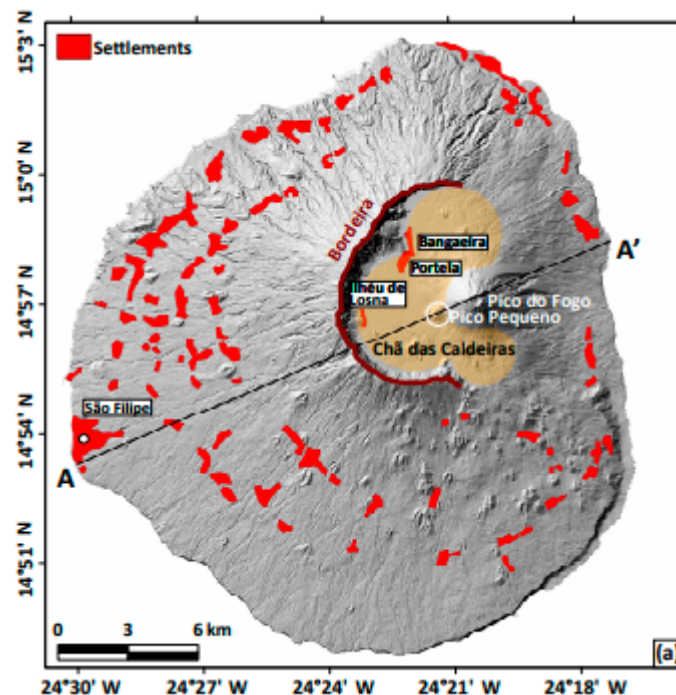


Figure 1. Map of Fogo Island [6].

The Sentinel-1A satellite was launched by the European Space Agency (ESA) on 3 April 2014. It has a C-band SAR antenna. Sentinel-1A acquires datasets with a new acquisition mode called the Terrain Observation and Progressive Scan (TOPS) mode, which is a modified form of ScanSAR mode. TOPS mode is very suitable for interferometric applications [8]. The Fogo volcano eruption episode was the first surface deformation activity acquired by Sentinel-1A since its launch. The datasets acquired by Sentinel-1A in TOPS mode during the volcano episode period is used for PSInSAR processing [9].

2. Dataset and Method

Seven scenes that Sentinel-1A acquired in Interferometric Wide (IW) TOPS mode, VV polarization acquired in ascending pass from 3 November 2014 to 15 March 2015, were used for this study. TOPS mode acquires data in three sub-swaths, covering a total swath of 250 km with a ground range cell size of 5×20 m. TOPS mode achieves a uniform Distributed Target Ambiguity Ratio and Signal-to-Noise Ratio by steering the radar beam from backwards to forwards electronically in an azimuth direction in addition to the steering of the beam in a range direction, as in normal ScanSAR mode. Each sub-swath is a collection of bursts where each burst is an independent Single Look Complex (SLC) image. In each sub-swath, these bursts are arranged in the

order of an azimuth-time domain, with black line separation in between the bursts. Before using the datasets for PSInSAR study, data preprocessing has to be done, which includes two steps. The first step is to extract the sub-swath covering the study area using the split operation, and the second step is the removal of the black strips in between the bursts by running a moving window averaging filter through all the bursts, called the deburst operation [8]. The dataset of 3 November 2014 was set as the master image and the remaining images were set as the slave images. The maximum spatial and temporal baselines to the master image were 92 metres and 132 days, respectively.

The process started by selecting the image of 3 November as the master image and all the remaining six slave images were coregistered with respect to the image taken as the master. Coregistration aligned the slave images with respect to the master image with sub-pixel-level accuracy. It was done to provide backscatter information from the same ground target. After coregistration, the interferograms were formed taking the phase difference between each slave and the master image. 'N' interferograms can be formed with 'N + 1' datasets. PSInSAR processing was done as per the flowchart shown in Figure 2.

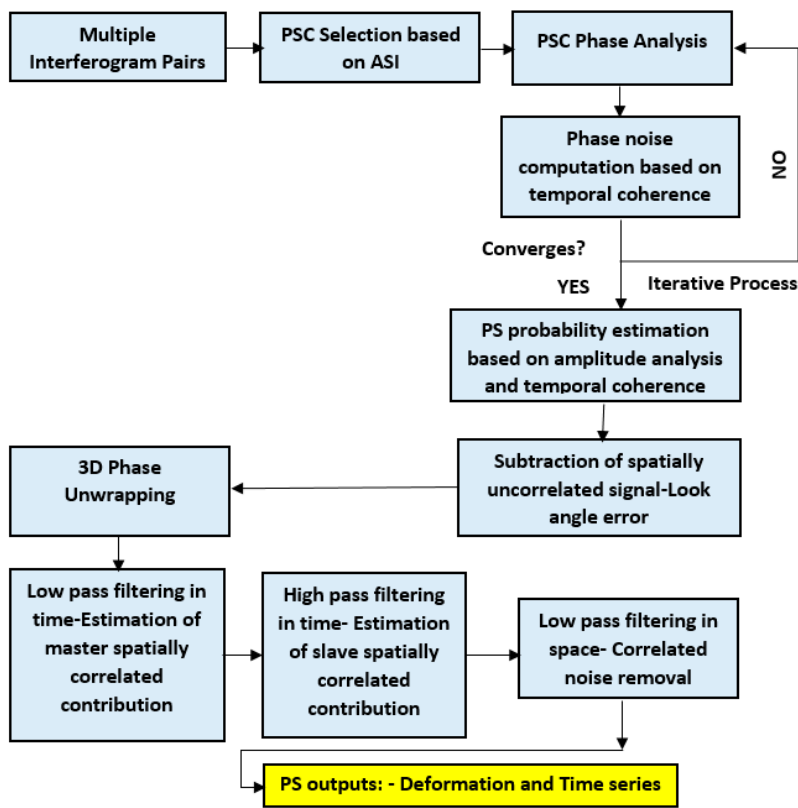


Figure 2. Process Flow Chart.

The Persistent Scatterers (PS) are the ground targets with high phase stability. The phase stability can be determined only after removing the undesired phase components, namely Atmospheric Phase Screen (APS), Digital Elevation Model (DEM) errors, terrain deformations and orbital ramps. Since targets with much less geometric and temporal decorrelation are required, pixels with stable amplitudes should be selected as Persistent Scatterer Candidates.

A subset of pixels from the Persistent Scatterer Candidates (PSCs) can be selected as the final Persistent Scatterers after estimating the phase stability of these pixels. The Amplitude Dispersion Index (D_A) is used to select the amplitude stable pixels [1,4,10].

$$D_A = \frac{\sigma_A}{\mu_A} \tag{1}$$

Equation (1) shows the formula for the Amplitude Dispersion Index. σ_A is the temporal standard deviation of each pixel in all the datasets and μ_A is the temporal mean of each pixel in all

the datasets. The amplitude dispersion and phase dispersion were in very good agreement for low values of the Amplitude Dispersion Index, approximately up to 0.25 [1]. The Amplitude Dispersion Index was used here to select the Persistent Scatterer Candidates for phase analysis, so a higher threshold of 0.4 was used here to select a large number of pixels.

Consider a PSC (x) in the i th interferogram, which is corrected for topographic errors. The interferometric phase of this PSC can be written as [4,11]:

$$\phi_{int,x,j} = W\{\phi_{def,x,i} + \phi_{a,x,i} + \phi_{orb,x,i} + \phi_{\varepsilon,x,i} + n_{x,i}\} \quad (2)$$

where $\phi_{def,x,i}$ is the surface deformation phase component, $\phi_{a,x,i}$ is the atmospheric phase delay component, $\phi_{orb,x,i}$ is the phase component due to orbital errors, $\phi_{\varepsilon,x,i}$ is the look angle errors phase component and $n_{x,i}$ is the noise. W represents the wrapped operator. The phase contributions due to the surface deformation, atmosphere and orbit were spatially correlated, so these three components were estimated using a filtering in spatial domain using a band-pass filter. The look angle error was estimated by correlating it with the perpendicular component of the baseline.

After correcting the spatially correlated phase components and the look angle error of all PSCs, the temporal coherence (γ) of all PSCs was calculated to estimate the phase noise level [4,11].

$$\gamma_x = \frac{1}{N} \left| \sum_{i=1}^N \exp\{\phi_{int,x,i} - \bar{\phi}_{int,x,i} - \Delta\hat{\phi}_{\varepsilon,x,i}\} \right| \quad (3)$$

Equation (3) represents the temporal coherence of a PSC (x), where N represents the number of interferograms, $\bar{\phi}_{int,x,i}$ is the estimated spatially correlated components and $\Delta\hat{\phi}_{\varepsilon,x,i}$ is the estimated look angle error. The PSC with high temporal coherence (γ_x) was selected as the new PSC and the remaining PSCs were rejected. All the first four phase components in Equation (2) were then re-estimated for this selected PSC and the process was repeated iteratively by dropping PSCs based on the above criteria until the last noise term of Equation (2) decreased and converged so that the temporal coherence of the PSC dominated the remaining small noise.

The Amplitude Dispersion Index and temporal coherence were used together to select the final set of Persistent Scatterers (PS) from the PSCs. For this requirement, Persistent Scatterer Probability was estimated for the PSC. At the last step, the PS points dominated by scatterers in neighbouring pixels and PS points persistent only in certain interferograms were discarded. The remaining pixels were chosen as the final Persistent Scatterers for surface deformation estimation [11].

Due to the spatially uncorrelated component of the look angle error, the interferometric phase difference between adjacent PS pixels may be greater than π . The slave and master contributions of the look angle error estimated earlier were removed from the wrapped phase before phase unwrapping [11].

The wrapped phase was then unwrapped using the 3D phase unwrapping technique. In the 3D phase unwrapping, two dimensions were in a spatial domain and one dimension was in the time domain. First phase differences of each PS pixel in the time domain had to be estimated and later spatial phase unwrapping was performed for each time step of a particular PS pixel using an iterative algorithm. Once the phase of each PS pixel was unwrapped in all the interferograms, it was then integrated in time. For accurate phase unwrapping, the deformation between a PS pixel and one of its neighbouring PS pixels should be less than half of the antenna wavelength either in space or time [11].

The unwrapped phase contained phase components due to the spatially correlated look angle error, atmosphere and orbital errors. These spatially correlated phase components had very low temporal coherence so they were estimated by using a high-pass phase filtering in the temporal domain followed by low-pass phase filtering in the spatial domain. The remaining interferometric phase contained the only phase due to surface deformation [11].

3. Results and Discussions

The PSInSAR technique was applied to seven Sentinel-1A SAR images acquired in the ascending pass from November 2014 to March 2015. From these datasets, six interferograms were

computed using the method described in the previous section. The Fogo volcano area was covered in the IW 2, so the PSInSAR method was applied with sub-swaths only.

Figure 3 shows the wrapped interferograms of each slave image with respect to the master image of 3 November 2014. The wrapped interferograms contain phase contributions due to the spatially correlated look angle error, atmosphere and orbital errors. From the interferogram of 27 November, it can be seen that, except for the Fogo volcano area, all other areas had broad interferogram fringes, indicating no surface deformation. The Fogo volcano area had discontinuous elliptical interferogram fringes, indicating surface deformations. The interferogram of 9 December shows the formation of circular discontinuous fringes, indicating the spreading of deformation to more areas. The interferograms of 21 December and 2 January show clear circular discontinuous interferogram fringes, showing the spread of deformation. Interferometric fringes in the interferograms of 14 January and 15 March are almost the same, indicating reduced volcanic activities.

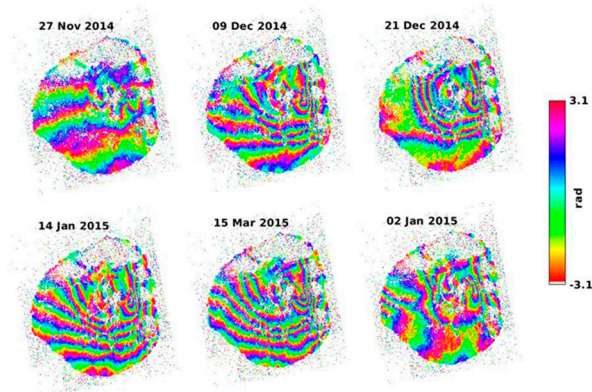


Figure 3. Wrapped Interferograms.

The unwrapped interferograms (Figure 4) justify the information extracted from the wrapped interferograms. The change in the phase of the interferograms can be observed from 27 November to 14 January, indicating surface deformation due to volcanic activities. In the interferogram of 27 November, the areas near the Fogo volcano have a yellow to cyan colour, indicating only very small phase change with respect to 3 November, except the volcano crater, which can be seen in the red colour in the middle of the image, indicating a high negative phase difference. The interferograms of 9 December and 21 December show a high phase difference at the volcano area indicated by the blue colour. High volcanic activity and the resulting lava flow was the reason for the high phase difference in these areas. From the interferogram of 2 January, it can be seen that the phase difference is considerably reduced, indicating reduced volcanic activity. But the interferogram of 14 January again shows a high phase difference at the volcano areas, indicating regained volcanic activities. The unwrapped interferograms of 14 January and 15 March are almost the same, indicating no surface deformation during this period and the halt of volcanic activities.

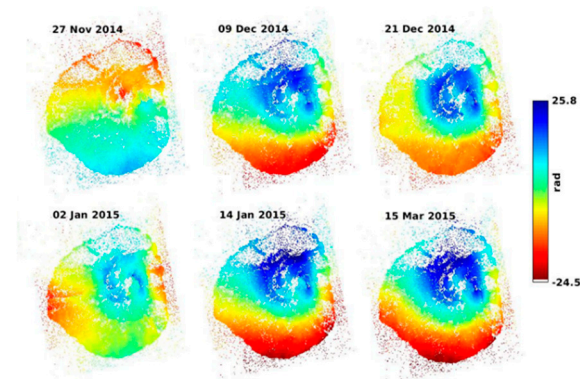


Figure 4. Unwrapped Interferograms.

Figure 5 shows the spatially correlated topographic phase component. It was estimated by the low-pass and high-pass filtering of the master and slave images, respectively. This estimated phase was then subtracted from the unwrapped phase of all interferograms to obtain the phase only due to surface deformation.

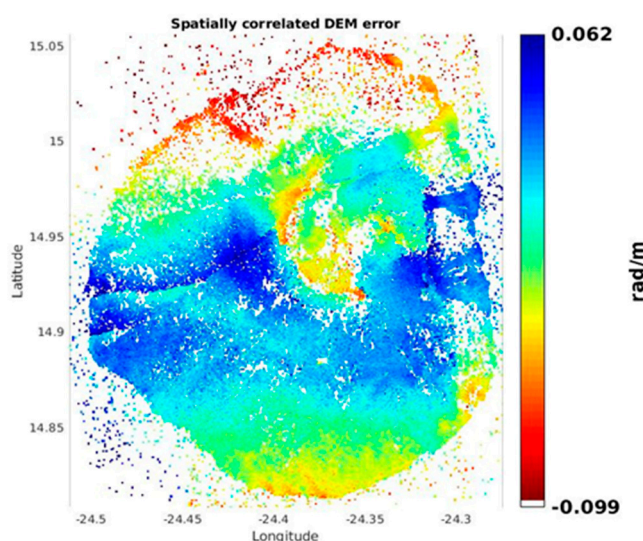


Figure 5. Spatially Correlated Topographic Phase.

The mean line-of-sight displacement (Figure 6) of the Fogo volcano area from 3 November to 15 March shows that there occurred a displacement of -3.45 cm at the Fogo Volcano crater due to the subsidence caused by volcanic activities, indicated by the red colour. The yellow- and cyan-coloured regions had a displacement of around 1 to 2 cm. The green colour indicates regions with zero displacements. Blue-coloured regions had a Line Of Sight (LOS) displacement of approximately $+3.5$ cm. The volcanic activity and lava flow occurred towards the northwestern regions of the volcano crater, indicating high LOS displacement towards these regions.

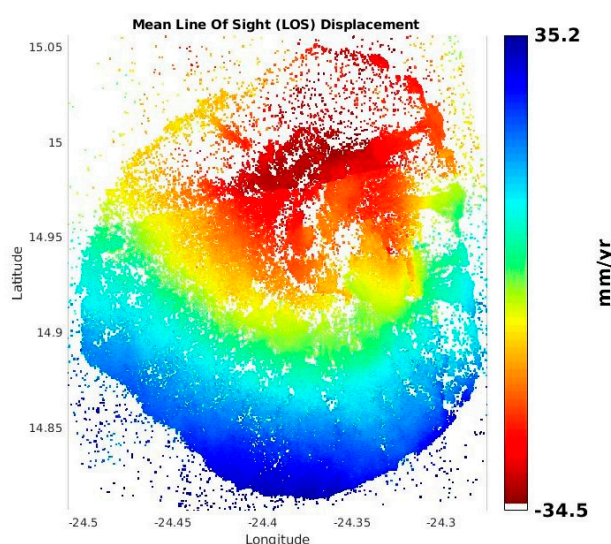


Figure 6. Mean LOS Displacement.

Figure 7 shows the standard deviation image of the mean LOS displacement. It can be seen that the areas in the red colour are less affected by the volcanic activities, indicated by the low standard deviation in the range of 2.2 cm/year. The low standard deviation was due to the low or near-similar displacement rate in different interferograms. The other areas had a high standard deviation

extending up to 3.0 cm/year due to the variation in displacement rate in different interferograms. The high standard deviation towards the northwestern side of the volcano crater, shown in the cyan and blue colours, indicates the varying displacement rates due to the lava flow where the Portela and Bangaeria villages are situated.

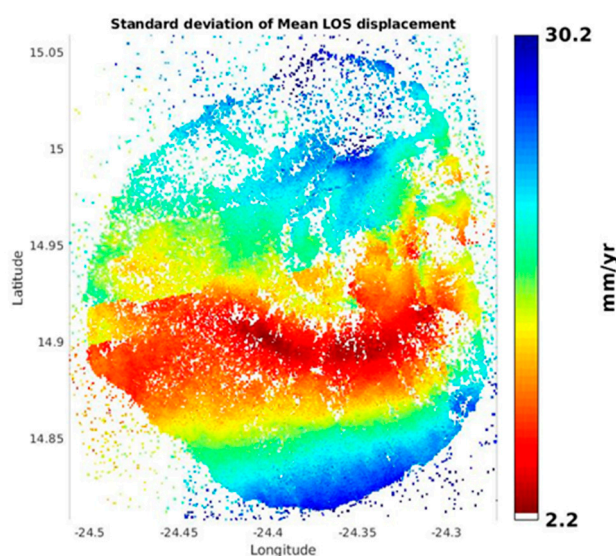


Figure 7. Standard Deviation of Mean LOS Displacement.

4. Conclusions

The surface deformation of Fogo volcano areas due to the volcanic eruption was estimated using the PSInSAR technique in this research. The PSInSAR technique used a large number of datasets to precisely estimate and remove the phase errors due to atmosphere and topography. The selection of PS pixels using both amplitude stability and phase stability ensured a high density of PS pixels. The natural terrain was free from any stable manmade structures. The absence of thick vegetation helped in preventing decorrelation of the interferograms. There occurred a displacement in the range of -34 mm to $+35$ mm to the Fogo volcano areas due to the volcanic episode. The high standard deviation of LOS displacement at the volcano areas indicates the deformation of the terrain.

Conflicts of Interest: The authors declare no conflict of interest.

References

1. Ferretti, A.; Prati, C.; Rocca, F. Permanent scatterers in SAR interferometry. *IEEE Trans. Geosci. Remote. Sens.* **2001**, *39*, 8–20.
2. Even, M.; Schulz, K. InSAR Deformation Analysis with Distributed Scatterers: A Review Complemented by New Advances. *Remote. Sens.* **2018**, *10*, 744.
3. Zebker, H.; Segall, P.; Kampes, B.; Hooper, A. A new method for measuring deformation on volcanoes and other natural terrains using InSAR persistent scatterers. *Geophys. Res. Lett.* **2004**, *31*, 1–5.
4. Hooper, A.; Segall, P.; Zebker, H. Persistent scatterer interferometric synthetic aperture radar for crustal deformation analysis, with application to Volcán Alcedo, Galápagos. *J. Geophys. Res. Space Phys.* **2007**, *112*.
5. Peltier, A.; Bianchi, M.; Kaminski, E.; Komorowski, J.-C.; Rucci, A.; Staudacher, T. PSInSAR as a new tool to monitor pre-eruptive volcano ground deformation: Validation using GPS measurements on Piton de la Fournaise. *Geophys. Res. Lett.* **2010**, *37*.
6. Richter, N.; Favalli, M.; de Zeeuw-van Dalssen, E.; Fornaciai, A.; da Silva Fernandes, R. M.; Pérez, N. M.; Levy, J.; Victória, S. S.; Walter, T. R. Lava flow hazard at Fogo Volcano, Cabo Verde, before and after the 2014–2015 eruption. *Nat. Hazards Earth Syst. Sci.* **2016**, *16*, 1925–1951.
7. Day, S.J.; Heleno da Silva, S.I.N.; Fonseca, J.F.B.D. A past giant lateral collapse and present-day flank instability of Fogo, Cape Verde Islands. *J. Volcanol. Geotherm. Res.* **1999**, *94*, 191–218.

8. Yague-Martinez, N.; Prats-Iraola, P.; Gonzalez, F.R.; Brcic, R.; Shau, R.; Geudtner, D.; Eineder, M.; Bamler, R. Interferometric Processing of Sentinel-1 TOPS Data. *IEEE Trans. Geosci. Remote. Sens.* **2016**, *54*, 1–15.
9. Gonzalez, P.J.; Bagnardi, M.; Hooper, A.J.; Larsen, Y.; Marinković, P.; Samsonov, S.; Wright, T. The 2014-2015 eruption of Fogo volcano: Geodetic modeling of Sentinel-1 TOPS interferometry. *Geophys. Res. Lett.* **2015**, *42*, 9239–9246.
10. Gonnuru, P.; Kumar, S. PsInSAR based land subsidence estimation of Burgan oil field using TerraSAR-X data. *Remote Sens. Appl. Soc. Environ.* **2018**, *9*, 17–25.
11. Ab Latip, A.S.; Matori, A.; Aobpaet, A.; Din, A.H.M. Monitoring of offshore platform deformation with stanford method of Persistent Scatterer (StaMPS). In Proceedings of the 2015 International Conference on Space Science and Communication (IconSpace), Langkawi, Malaysia, 10–12 August 2015; pp. 79–83.



© 2019 by the authors. Licensee MDPI, Basel, Switzerland. This article is an open access article distributed under the terms and conditions of the Creative Commons Attribution (CC BY) license (<http://creativecommons.org/licenses/by/4.0/>).